

Magnetic Field Amplification in Tycho and other Shell-type Supernova Remnants

H.J. Völk^a, E.G. Berezhko^b and L.T. Ksenofontov^b

(a) Max-Planck-Institut für Kernphysik, Postfach 103980, D-69029, Heidelberg, Germany

(b) Yu.G.Shafer Institute of Cosmophysical Research and Aeronomy, 31 Lenin Ave., 677980 Yakutsk, Russia

Presenter: H.J. Völk (Heinrich.Voelk@mpi-hd.mpg.de), ger-voelk-H-abs1-og14-oral

It is shown that amplification of the magnetic field in supernova remnants (SNRs) occurs in all seven objects where morphological measurements are presently available in the hard X-ray continuum at several keV. For the three archetypical objects (SN 1006, Cas A and Tycho's SNR) to which nonlinear time-dependent acceleration theory has been successfully applied up to now, the global theoretical and the local observational field strengths agree very well, suggesting that all young SNRs exhibit the amplification effect as a result of very efficient acceleration of nuclear cosmic rays (CRs) at the outer shock. A fourth such case is presented elsewhere in these Proceedings for the remnant of Kepler's SN, with the same conclusion. We consider field amplification as a measure of nuclear CR acceleration. The above results are also used to investigate the time evolution of field amplification in young SNRs. They rather clearly show that the ratio of the magnetic field energy density and the kinetic energy density of gas flow into the shock is of the order of a few percent if the shock speed is high enough, $V_s > 10^3$ km/s. It implies that the escape of the highest energy nuclear particles from their sources becomes progressively important with age, reducing also the cutoff in the π^0 -decay gamma-ray emission spectrum with time after the end of the sweep-up phase.

1. Introduction

Recent observations with the *Chandra* and *XMM-Newton* X-ray space telescopes have confirmed earlier detections of nonthermal continuum emission in hard X-rays from young shell-type supernova remnants (SNRs). With *Chandra* it became even possible to resolve spatial scales down to the arcsec extension of individual dynamical structures like shocks. The results have been evaluated in [1]. Very recently the SNR Vela Jr. (RX J0852.0-4622, G266.6-1.2) has been added to this list [2]. These results can be seen from three different viewpoints: First of all, assuming the filamentary structures to represent synchrotron emission near shocks, their de-projected brightness profile can be considered as the synchrotron cooling length to derive the effective downstream magnetic field strength B_d (e.g. [3, 4, 5]). Secondly, we can compare this B_d with the amplified B_d -values predicted in [6] for the interior magnetic field strength that make a complete dynamical model of the SNR consistent with the spatially integrated synchrotron spectrum from the radio range to hard X-rays. The third viewpoint is from the plasma physics of field amplification in an ionized gas with a very strong nuclear cosmic ray (CR) gradient, which makes these results theoretically plausible [7]. We shall summarize the field amplification results here and present in particular an improved prediction for the gamma-ray spectral energy distribution in Tycho's SNR. Finally, we discuss the ratio of the magnetic field energy density and the kinetic energy density of gas in the different objects.

2. Results and discussion

As shown earlier [5], the width $L \approx 7l_2$ of the observable synchrotron brightness profile of a SNR is always appreciably wider than the downstream width l_2 in radius r of the three-dimensional emissivity, simply for geometric reasons. The length-scale l_2 is the distance through which the very energetic electrons stream away

from the shock during a synchrotron loss time $\tau(p) = 9m_e^2 c^2 / (4r_0^2 B_d^2 p)$, where m_e is the electron mass, $r_0 \approx 10^{-13}$ cm is the classical electron radius, c denotes the speed of light, and B_d is the effective magnetic field in the downstream region. For given frequency ν the momentum p of the radiating electron is approximately given as $p \propto \sqrt{\nu/B_d}$.

In the limit of a strongly fluctuating magnetic field around the shock on all scales, we assume that the diffusion coefficient $\kappa(p)$ is given by the Bohm limit, $\kappa(p) = \rho_B v / 3$, where ρ_B and v are the particle gyroradius and velocity, respectively. Then l_2 is determined by B_d and ν which can be conveniently turned into an equation for B_d in terms of l_2 and ν :

$$B_d = [3m_e^2 c^4 / (4e r_0^2 l_2^2)]^{1/3} (\sqrt{1 + \delta^2} - \delta)^{-2/3}, \quad (1)$$

with

$$\delta^2 = 0.12 [c / (r_0 \nu)] [V_s / (\sigma c)]^2, \quad (2)$$

where e is the proton charge. It is simple to verify that for the considered X-ray energies, which lie in the cutoff region of the integrated synchrotron brightness, for most sources the case of strong losses [8] is relevant, where the emissivity width is given by the limiting cases of Eqs.(1, 2):

$$l_2 = \sqrt{\kappa_2 \tau_2}, \quad (3)$$

i.e. by the postshock *diffusion length* in a synchrotron loss time. The radial emissivity profile is parametrized by B_d alone in this limit.

Regarding Tycho's SNR, for the *global determination* of the effective downstream field B_d we compared the theoretical synchrotron spectrum with the observed *spatially integrated* spectrum. To explore the possible bandwidth of B_d -values we approximated the data with a slightly softer radio spectrum than adopted earlier [9]. In the framework of the strongly nonlinear system of equations, the required stronger shock modification by the nuclear component is achieved by a somewhat increased proton injection rate. The theoretically implied increase of the magnetic field from 240 to 360 μ G then requires a reduction of the amplitude of the electron momentum distribution since the radio electrons are not subject to synchrotron cooling at the present epoch. The optimum magnetic field strength lies between the two cases, roughly at 300 μ G. This leads to an optimum value $B_d \approx 300 \pm 60 \mu$ G from acceleration theory. Apart from profiles given in the literature (e.g. [11]), we have investigated *Chandra* X-ray images in the north and northwest, obtained for X-ray energies $4 < \epsilon_\nu < 6$ keV with the ACIS spectroscopic array from the *Chandra* archive, using the morphology template of eq.(1). This corresponds to 6 profiles through the remnant's outer boundary. After co-adding the profiles, the average profile determines a mean value of $B_d = 273 (+49 - 37) \mu$ G with very high fitting quality which agrees rather well with the optimized field value from acceleration theory. We take the latter as our preferred value.

For completeness we shall also give the resulting prediction for the total integral γ -ray energy flux from Tycho's SNR for the above extreme values of B_d , equal to 240 μ G and 360 μ G, respectively, for the same gas density $N_H = 0.5 \text{ cm}^{-3}$ (Fig. 1). Compared to the earlier prediction [9], the hadronic π^0 -decay flux changes very little, as expected, whereas the Inverse Compton flux changes by a factor of about 7 between 240 μ G and 360 μ G in effective magnetic field strength, given the observed synchrotron flux. Thus, a detection of Tycho's SNR in TeV gamma rays close to the predicted hadronic flux would again indicate a hadronic CR source - as the entire discussion in terms of acceleration theory implies in any case.

The hadronic γ -ray emission is quite sensitive to the ambient gas density which may not have been fixed sufficiently well yet from radio observations. We note however that the nominal value for the mean ambient hydrogen density $N_H = 0.5 \text{ cm}^{-3}$, chosen in Fig. 1 is on the low rather than on the high side.

For the other SNRs where both local profiles and a global theoretical acceleration model exist (SN 1006,

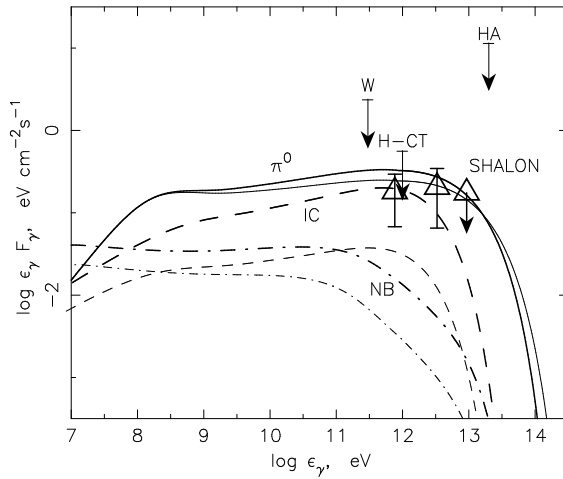


Figure 1. Predicted γ -ray spectral energy distribution, as a function of γ -ray energy: IC emission (*dashed lines*), Nonthermal Bremsstrahlung (NB, *dash-dotted lines*), and π^0 -decay (*solid lines*). The observed 3σ γ -ray upper limits (W - Whipple, H-CT - HEGRA IACT system, and the 95% confidence HA - HEGRA AIROBICC upper limit) are shown together with the detection/upper limit claimed by the Shalou group. *Thick lines* correspond to a downstream field of $B_d = 240 \mu\text{G}$, whereas *thin lines* stem from assuming the maximum field value $B_d = 360 \mu\text{G}$.

Cas A, Kepler's SNR), the agreement between both methods to determine B_d is of a similar quality. All these objects are predicted to be hadronically dominated γ -ray sources. More difficult are the cases of RCW 86 and RX J1713.7-3946, where the *Chandra* profiles are not obviously at the rim. This makes the de-projection uncertain, even though the interpretation of the filaments in terms of shock transitions leads in both cases still to significant field amplification [1]. Therefore we have for both sources allowed for a range of de-projection factors in Fig. 2 below.

Regarding the magnetic field strengths derived we can attempt to learn something from these results by empirically correlating the magnetic field pressure $B_d^2/(8\pi)$ with the ram pressure $\rho_0 V_s^2$ of the upstream gas in the shock frame of reference. Assuming that $B_d^2/(8\pi)$ reaches some fraction of the CR pressure P_c at the shock, and assuming very efficient acceleration so that $P_c = \epsilon \rho_0 V_s^2$, with $\epsilon = O(1)$, we expect a constant ratio $B_d^2/(8\pi \rho_0 V_s^2)$ as a function of shock velocity V_s for an individual object. This appears to us to be the physically most natural result, given the overall dynamics in the shock (see also the discussion in [9]). It is useful to represent the ratio of magnetic and kinetic energy densities in the form:

$$\frac{B_d^2/(8\pi)}{\rho_0 V_s^2} \approx 1.7 \times 10^{-2} \left\{ \frac{[B_d/(100 \mu\text{G})]^2}{[N_H/(1 \text{ cm}^{-3})][V_s/(10^3 \text{ km/s})]^2} \right\}. \quad (4)$$

We have not included a data point for Vela Jr. in Fig. 2, since we do not yet have a model for it which fulfills all observational constraints, claimed in the literature to exist. However, all possible scenarios lead to a substantial field amplification with B_d in excess of $100 \mu\text{G}$.

The present uncertainties in the data, which are not more accurate than 25% and cover only a rather limited range of the shock speed V_s , do not allow a distinction between a constant ratio $B_d^2/(8\pi \rho_0 V_s^2)$ and one with a linear growth of $B_d^2/(8\pi \rho_0 V_s^2)$ with V_s . However, the data are highly likely to exclude a decrease of $B_d^2/(8\pi \rho_0 V_s^2)$ with increasing V_s . Obviously this means that with growing age, that is decreasing shock velocity, the field amplification in SNRs decreases about linearly with the shock velocity. Fig. 2 indicates that in all young SNRs with large enough shock speed $V_s > 10^3 \text{ km/s}$ the effective (amplified) magnetic field energy density is near $B_d^2/(8\pi) = 3.5 \times 10^{-2} \rho_0 V_s^2$.

We thus tentatively conclude that field amplification is confined to young remnants. This also implies that the escape of the highest energy nuclear particles, accelerated at an earlier epoch with high effective field, becomes progressively important as the remnant age increases. This implies a lower and lower cutoff of the resulting

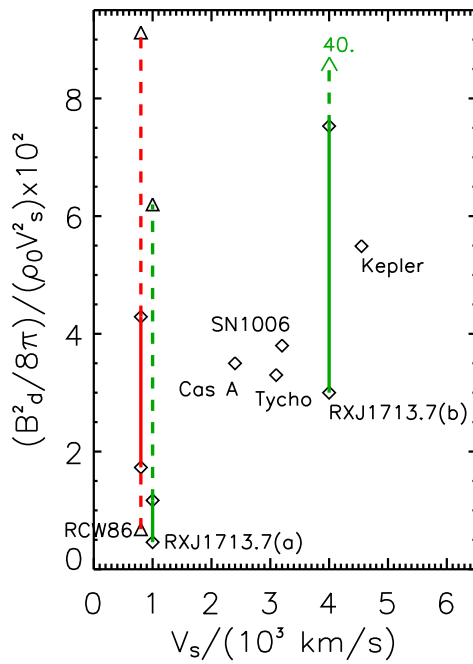


Figure 2. Ratio of downstream magnetic field pressure to preshock gas ram pressure vs. shock velocity V_s for six young SNRs that show field amplification. For the objects RCW 86 and RX J1713.7-3946 a range of normalized magnetic field pressures is given. (For RCW 86 the four points correspond to $L/l_2 = 1, 2, 4$ and 7 , respectively, and the *solid vertical line segment* corresponds to the assumed range of uncertainty $7/4 < 7l_2/L < 7/2$. For RX J1713.7-3946 the three points correspond to $L/l_2 = 1, 2$ and 7 , respectively, and the *solid vertical line segment* corresponds to the uncertainty range $7/2 < 7l_2/L < 7$) For this remnant two alternative shock states are depicted: the low velocity case (a) corresponds rather to the cloudy medium in the north and west of the remnant. The high velocity case (b) is more representative for the very low density regions in the southern projection of the remnant, the fully projected case $L/l_2 = 7$ corresponding to a value of 40, out of scale in the figure.

γ -ray spectrum from a SNR with age. As a result, the highest energy nuclear particles are to be found in SNRs that have just reached the Sedov phase. Older remnants are increasingly unable to confine them.

The amplified magnetic field also leads to a depression of the Inverse Compton and nonthermal Bremsstrahlung γ -ray emission relative to the hadronic emission for young remnants, given the synchrotron emission. Nevertheless the hadronic γ -ray emission depends strongly on N_H , essentially $\propto N_H^2$ [12]. Thus a strong source of nuclear CRs can still be a γ -ray source with a comparable or even preponderant IC emission. Ultimately even SN 1006 might turn out as an example for that case, since its N_H must be quite small .

References

- [1] H.J. Völk, E.G. Berezhko, L.T. Ksenofontov, A&A 433, 229 (2005).
- [2] A. Bamba, R. Yamazaki, J.S. Hiraga, astro-ph/0506331 (2005).
- [3] J. Vink, J.M. Laming, ApJ 548, 758 (2003).
- [4] E.G. Berezhko, L.T. Ksenofontov, H.J. Völk, A&A 412, L11 (2003).
- [5] E.G. Berezhko, H.J. Völk, A&A 419, L27 (2004).
- [6] E.G. Berezhko, L.T. Ksenofontov, H.J. Völk, A&A 395, 943 (2002).
- [7] A.R. Bell, MNRAS 353, 550 (2004).
- [8] H.J. Völk, G.E. Morfill, M.A. Forman, ApJ 249, 161 (1981).
- [9] H.J. Völk, E.G. Berezhko, L.T. Ksenofontov, G.P. Rowell, A&A 396, 649 (2002).
- [10] E.G. Berezhko, H.J. Völk, A&A 427, 525 (2004).
- [11] U. Hwang, A. Decourchelle, S.S. Holt, R. Petre, R., ApJ 581, 1101 (2002).
- [12] L.T. Ksenofontov, E.G. Berezhko, H.J. Völk, A&A submitted (2005).